5-1986

# ULF/ELF electromagnetic fields generated along the sea floor interface by a straight current source of infinite length

Aziz S. Inan
*University of Portland*, ainan@up.edu

A. C. Fraser-Smith

O. G. Villard Jr.

Citation: Pilot Scholars Version (Modified MLA Style)

Inan, Aziz S.; Fraser-Smith, A. C.; and Villard, O. G. Jr., "ULF/ELF electromagnetic fields generated along the sea floor interface by a straight current source of infinite length" (1986). *Engineering Faculty Publications and Presentations*. 3.
http://pilotscholars.up.edu/egr_facpubs/3

# ULF/ELF electromagnetic fields generated along the seafloor interface by a straight current source of infinite length

*A. S. Inan,*[1] *A. C. Fraser-Smith, and O. G. Villard, Jr.*

Space, Telecommunications and Radioscience Laboratory, Stanford University, California

Propagation of ULF/ELF electromagnetic fields along the seafloor interface (assumed to be a plane boundary separating two semi-infinite conducting media) is considered. Earlier expressions for the electromagnetic fields generated by a straight current source of infinite length are applied to the sea/seabed interface. The field components are calculated numerically and are compared to the field components in seawater of infinite extent. At the seafloor boundary, the fields can propagate longer distances because of the lower seabed conductivities. The new horizontal component of the magnetic field generated as a result of the existence of the sea/seabed interface becomes larger than the vertical component of the magnetic field at large distances; it is also more sensitive to the conductivity of the seabed at low frequencies. The results indicate that there is an optimal frequency at which two of the field components have a maximum field intensity at a certain distance from the source. Some practical applications are discussed.

## 1. INTRODUCTION

Electromagnetic wave propagation in conducting media has been of practical interest since the beginning of this century. Toward the end of the first World War, limited experimental and theoretical work focused on the generation of electromagnetic fields in, on, and above the sea by submerged cables carrying alternating current [*Drysdale*, 1924; *Butterworth*, 1924]. This work was motivated by the use of cable-generated electromagnetic fields for navigation [*Wright*, 1953]. These fields have also become important for communicating with submarines [*Moore*, 1951, 1967]. Despite the absorption of electromagnetic energy in seawater, electromagnetic signals at ELF are able to propagate to moderately great distances in the ocean and, as a result, they are a possible means of communication with deeply submerged submarines [*Wait*, 1972]. A more recent application is geophysical prospecting. A significant amount of research has used electromagnetic techniques to study the structure of the earth's crust [*Burrows*, 1963; *Wait and Spies*, 1972a, b, c]. Propagation of VLF signals through the earth has also been of considerable interest for mine communi-

cation; in the event of a mine disaster, telephone wires and other normal links of communication could be interrupted, but communication with the trapped miners could still be achieved through the earth [*Wait and Spies*, 1973].

The first extensive theoretical study of electromagnetic wave propagation between submerged stations in seawater was reported by *Moore* [1951], and most of the subsequent theoretical work centered on a sea of infinite extent [*Wait*, 1952; *Kraichman*, 1976] or on the effects of the sea surface in a very deep sea [*Moore*, 1951; *Wait and Campbell*, 1953; *Hansen*, 1963; *Banos*, 1966; *Fraser-Smith and Bubenik*, 1976; *Bannister and Dube*, 1977]. These studies indicated that if the horizontal distance between the source and observer is larger than several skin depths, the energy received may follow an up-over-down mode above the surface [*Moore and Blair*, 1961]. This result led to the conclusion that near the sea/seabed interface, the energy received may follow an analogous down-under-up mode in a weakly conducting seabed under certain conditions [*Bubenik and Fraser-Smith*, 1978].

Such a mode has been investigated in a somewhat different context by a number of researchers [*Wheeler*, 1960; *Burrows*, 1963; *Mott and Biggs*, 1963; *Wait and Spies*, 1972a, b, c; *King and Smith*, 1981]. These studies suggested that a waveguide may exist under both the sea and continents and that it may become a usable communication link if other above-ground communications are disrupted; it would also have

[1] Now at Engineering Department, San Francisco State University, California.

much lower noise levels. In an electrically shallow sea, the sea-surface and seabed modes may exist simultaneously. *Weaver* [1967] analyzed the fields of electric dipoles submerged in seawater, and *Ramaswamy et al.* [1972] considered a submerged horizontal magnetic dipole, both taking a sea of one skin depth deep. Ramaswamy also computed the field components when both the source and receiver are located at the sea/seabed interface as a function of seawater induction number varying from 0 to 3. Numerical data [*Bubenik and Fraser-Smith*, 1978; *Fraser-Smith and Bubenik*, 1979] of the electromagnetic fields produced by a vertical magnetic dipole submerged in a sea of finite depth reveal the effects of a strongly conducting seabed. Other electromagnetic methods for obtaining seabed conductivities have been proposed [*Brock-Nannestad*, 1965; *Bannister*, 1968a, b; *Coggon and Morrison*, 1970]. *Bannister* [1968a] observed that the conductivity of the seabed may be determined by measuring only the horizontal component of the magnetic field produced at the sea/seabed interface by a long horizontal line source located at the air/sea interface. *Coggon and Morrison* [1970] considered a vertical magnetic dipole submerged in seawater and analyzed the electromagnetic fields over various ranges of seawater induction numbers and seabed conductivities. A recent active-source electromagnetic sounding experiment on the ocean floor [*Young and Cox*, 1981] introduced new possibilities for studying the electrical conductivity of the ocean crust.

This work considers an electrically deep sea and calculates the electromagnetic fields produced by a long straight insulated cable when the source and receiver are both located on the seafloor. The effects of the sea surface are neglected because attenuation on the paths of propagation from the cable to the receiver via the sea surface is larger. Both the sea and seabed are assumed to be isotropic, homogeneous, and time-invariant conducting media separated by a plane interface—the seafloor. Frequencies in the ULF/ELF band (less than 3 kHz) are considered because only signals in these bands will propagate to ranges of interest before being significantly attenuated. The displacement current terms in both media are neglected, and this assumption is well justified in these frequency ranges. It is assumed that both media are nonmagnetic, with permeabilities equal to the free-space permeability ($\mu_0 = 4\pi \times 10^{-7}$ H/m). The conductivity of the seawater $\sigma_s$ is assumed to be 4 S/m and the conductivity of the seabed varies.

If the length of a long straight insulated cable lying at the plane interface of two conducting media is longer than the longest of all other physical dimensions, it is known as an "infinite" cable. There is an alternating current $I \cos \omega t$ flowing in the cable which is assumed to be uniformly distributed, and this assumption is justified at sufficiently low frequencies [*Wait*, 1952; *Sunde*, 1968]. The cable is oriented along the x-axis, and the plane interface of the two media is $z = 0$. The direction of the current is out of the paper at $t = 0$. Everything is invariant in the x-direction, as illustrated in Figure 1.

It is assumed that all the fields vary with time as exp ($j\omega t$). The electric and the magnetic field components for the infinite cable are calculated from explicit expressions and numerical integration [*Wait*, 1953; *Inan et al.*, 1982]. Most of the data are presented in dimensionless form by measuring all distances in terms of the skin depth of the seawater $\delta_s$ defined as

$$\delta_s = (2/\omega\mu_0 \sigma_s)^{1/2}$$

where $\omega$ is the angular frequency related to frequency f by the relation $\omega = 2\pi f$. Seabed conductivity is normalized to seawater conductivity by $\sigma' = \sigma_f/\sigma_s$, where $\sigma'$ is the normalized seabed conductivity. The skin depth in the seabed is related to the skin depth in sea water by $\delta_f = \delta_s/(\sigma')^{1/2}$, and the wavelengths $\lambda_{(s,f)}$ in both media are proportional to the skin depths, since

$$\lambda_{(s,f)} = 2\pi\delta_{(s,f)}$$

In conducting media, field intensity varies with an exponential term $e^{-d/\delta}$ (where $d$ is the distance from the source) representing 55 dB/wavelength attenuation [*Hansen*, 1963], and it is this attenuation that limits the range of the electromagnetic signal. Figure 2 is a logarithmic plot of skin depth, wavelength, and exponential attenuation in sea water as a function of frequency.

The numerical results obtained in this work can be used to determine effective sea-bed conductivities in
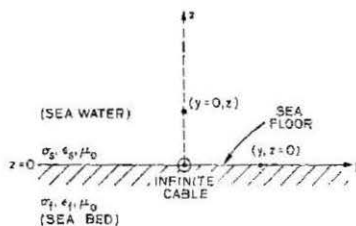


Fig. 1.   Infinite cable located at the sea/floor interface. Note the symmetry with respect to the x-axis.

smooth regions of the seafloor. Stretches of the abyssal plain in the western North Atlantic have been measured to be smooth within 2 m over distances of 100 km [*Pickard and Emery*, 1982]. It is also assumed that the seawater shields the seafloor from atmospheric noise and, because the region of interest is far from the shore, the possibility of atmospheric and power-line noise propagating through the earth's crust can be neglected. This is important because atmospheric noise is especially strong in the ULF/ELF frequency ranges [*Liebermann*, 1962; *Soderberg*, 1969]. The only other likely source of noise is the internal noise of the receiver; the other natural electromagnetic sources of noise will not be as significant [*Chave and Cox*, 1982].

## 2. FIELD COMPONENTS

Following *Wait*'s [1961] work, the field components produced by an infinite cable lying along the x-axis can be written

$$E_{s,x} = \frac{-j\omega\mu_0 I}{\pi} \int_0^\infty \frac{e^{-u_s z}}{u_s + u_f} \cos(\lambda y) \, d\lambda \quad (1)$$

$$B_{s,y} = \frac{-\mu_0 I}{\pi} \int_0^\infty \frac{u_s e^{-u_s z}}{u_s + u_f} \cos(\lambda y) \, d\lambda \quad (2)$$

$$B_{s,z} = \frac{\mu_0 I}{\pi} \int_0^\infty \frac{\lambda e^{-u_s z}}{u_s + u_f} \sin(\lambda y) \, d\lambda \quad (3)$$

with $B_{s,x} = E_{s,y} = E_{s,z} = 0$, and where

$$u_s = \sqrt{\lambda^2 + \gamma_s^2} \qquad u_f = \sqrt{\lambda^2 + \gamma_f^2}$$

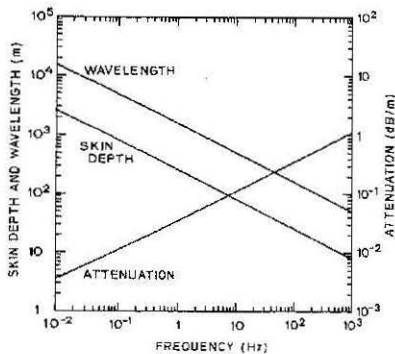$$\gamma_s^2 = j\omega\mu_0\sigma_s \qquad \gamma_f^2 = j\omega\mu_0\sigma_f$$



Fig. 2. Skin depth, wavelength, and exponential attenuation in seawater with a conductivity of 4 S/m (based on Figure A.3 by *Kraichman* [1976]).

These expressions can also be written in the dimensionless form

$$E_{s,x}^p = \frac{\pi\sigma_s\delta_s^2}{I} E_{s,x} = -\lim_{z'\to 0} j2 \int_0^\infty \frac{e^{-u_s'z'}}{u_s' + u_f'} \cos(\lambda' y') \, d\lambda' \quad (4)$$

$$B_{s,y}^p = \frac{\sqrt{2}\pi\delta_s}{\mu_0 I} B_{s,y} = -\lim_{z'\to 0} \sqrt{2} \int_0^\infty \frac{u_s' e^{-u_s'z'}}{u_s' + u_f'} \cos(\lambda' y') \, d\lambda' \quad (5)$$

$$B_{s,z}^p = \frac{\sqrt{2}\pi\delta_s}{\mu_0 I} B_{s,z} = \lim_{z'\to 0} \sqrt{2} \int_0^\infty \frac{\lambda' e^{-u_s'z'}}{u_s' + u_f'} \sin(\lambda' y') \, d\lambda' \quad (6)$$

where

$$u_s' = \sqrt{\lambda'^2 + j2}, \qquad u_f' = \sqrt{\lambda'^2 + j2\sigma'}$$

and $z' = z/\delta_s$, $y' = y/\delta_s$, $\lambda' = \lambda\delta_s$, and $\sigma' = \sigma_f/\sigma_s$.

When the receiver is located at the interface $z = 0$, two of the field components can be expressed in an explicit form derived by *Wait* [1953, 1962] as

$$E_{s,x} = \frac{j\omega\mu_0 I}{\pi(\gamma_f^2 - \gamma_s^2)y^2} \left[ \gamma_s y K_1(\gamma_s y) - \gamma_f y K_1(\gamma_f y) \right] \quad (7)$$

$$B_{s,z} = \frac{\mu_0 I}{\pi(\gamma_f^2 - \gamma_s^2)y^3} \left[ 2\gamma_s y K_1(\gamma_s y) + \gamma_s^2 y^2 K_0(\gamma_s y) \right.$$
$$\left. - 2\gamma_f y K_1(\gamma_f y) - \gamma_f^2 y^2 K_0(\gamma_f y) \right] \quad (8)$$

where $K_0$ and $K_1$ are the modified Bessel functions of the second kind of order zero and one with complex arguments. The horizontal component of the magnetic field $B_{s,y}$ does not have an explicit expression. When $\omega = 0$, both $E_{s,x}$ and $B_{s,y}$ become zero and the vertical magnetic field component simplifies to

$$B_{s,z} = \frac{\mu_0 I}{2\pi y}$$

## 3. NUMERICAL RESULTS

This section presents the numerical data for the electric and magnetic field components at the interface of the two conducting media. Two of these components $E_{s,x}$ and $B_{s,z}$ have explicit expressions (equations (7) and (8)) that can be expressed in terms of Kelvin functions [*Young and Kirk*, 1964] and their derivatives. After some algebraic manipulations, their amplitudes can be written in dimensionless form as

$$|E_{s,x}^p| = \frac{\pi\sigma_s\delta_s^2}{I} |E_{s,x}| = \frac{2}{(1 - R^2)\alpha_s}$$
$$\cdot \left[ (c_1 - Rc_2)^2 + (d_1 - Rd_2)^2 \right]^{1/2} \quad (9)$$

and

$$|B_{s,z}^p| = \frac{\sqrt{2\pi}\delta_s}{\mu_0 I} |B_{s,z}| = \frac{2}{(1-R^2)\alpha_s^2}$$
$$\cdot [(\alpha_s(a_1 - R^2 a_2) - 2(d_1 - Rd_2))^2$$
$$+ (\alpha_s(b_1 - R^2 b_2) + 2(c_1 - Rc_2))^2]^{1/2} \quad (10)$$

where

$$a_1 = ker_0\,\alpha_s \qquad a_2 = ker_0\,\alpha_f$$
$$b_1 = kei_0\,\alpha_s \qquad b_2 = kei_0\,\alpha_f$$
$$c_1 = ker_0'\,\alpha_s \qquad c_2 = ker_0'\,\alpha_f$$
$$d_1 = kei_0'\,\alpha_s \qquad d_2 = kei_0'\,\alpha_f$$

and

$$\alpha_s = \sqrt{2}y' \qquad \alpha_f = R\alpha_s \qquad R^2 = \sigma' = \sigma_f/\sigma_s$$

where $\alpha_s$ and $\alpha_f$ are defined as the induction numbers in the seawater and seabed respectively [Coggon and Morrison, 1970]. The above expressions for the horizontal electric field component and the vertical magnetic field component can be calculated numerically by using tables of Kelvin functions and their derivatives [Lowell, 1959].

The other nonzero component at the interface is the horizontal magnetic field component $B_{s,y}$, and it can be computed only by numerical integration. The expression for it (equation (5)) can be divided into two parts,

$$B_{s,y}^p = -\sqrt{2}\int_0^{\lambda_{max}'} \frac{u_s'}{u_s' + u_f'}\cos(\lambda'y')\,d\lambda'$$
$$- \lim_{z'\to 0}\sqrt{2}\int_{\lambda_{max}'}^{\infty} \frac{u_s'e^{-u_s'z'}}{u_s' + u_f'}\cos(\lambda'y')\,d\lambda'$$

Two factors must be determined for numerical integration. The first is $\lambda_{max}'$. It is assumed that the effective conductivity of the seafloor is smaller than that of seawater ($\sigma' < 1$). The value for $\lambda_{max}'$ is chosen such that $\lambda_{max}'^2 \gg 2$ and, if this constraint is satisfied, both $u_s'$ and $u_f'$ can be approximated as

$$u_s' \simeq \lambda' \qquad u_f' \simeq \lambda'$$

for $\lambda' > \lambda_{max}'$. Based on this approximation, the second integral above can be replaced by an explicit term yielding

$$B_{s,y}^p = -\sqrt{2}\int_0^{\lambda_{max}'} \frac{u_s'}{u_s' + u_f'}\cos(\lambda'y')\,d\lambda' + \frac{\sin(\lambda_{max}'y')}{\sqrt{2}y'} \quad (11)$$

Similarly the integral expression for the vertical component of the magnetic field (equation (6)) can be

written as

$$B_{s,z}^p = \sqrt{2}\int_0^{\lambda_{max}'} \frac{\lambda'}{u_s' + u_f'}\sin(\lambda'y')\,d\lambda' + \frac{\cos(\lambda_{max}'y')}{\sqrt{2}y'} \quad (12)$$

The above integrands can be separated into their real and imaginary parts and be numerically integrated as real integrals. The data for the field components can then be obtained by recombining these terms according to (11) and (12). The second factor is the method of integration. Both integrands are well-behaved functions except for the cosine or sine term that may oscillate rapidly at greater distances than the skin depth of the seawater [Hermance and Peltier, 1970]. Two techniques of numerical integration, Weddle's rule [Computation Laboratory of Harvard University, 1949] and Filon's method [Tranter, 1956] were used; by selecting the integration interval small enough, both produce sufficiently accurate results.

The computations can be verified in several ways. The first one is to compare the results obtained by the two different numerical integration techniques. The second is to compare the results obtained for $B_{s,z}$ through numerical integration using (12) to the results obtained for the same component using (10) and tables of Kelvin functions. The third is to check the results by using the approximate expressions for the lower and higher frequency ranges.

The first panels in Figures 3, 4, 5, and Figure 6 show the variations in the parametric amplitudes of the three nonzero field components $E_{s,x}^p$, $B_{s,y}^p$, and $B_{s,z}^p$ and the total magnetic field $B_{s,T}^p$ with the induction number of seawater $\alpha_s$. Note that the parametric terms $\pi\sigma_s\delta_s^2/I$ and $2^{1/2}\pi\delta_s/\mu_0 I$ appearing on the left-hand side depend on frequency $f$ and not on receiver distance $y$. These curves can be used for any frequency in the valid frequency range. The horizontal axis indicates the perpendicular distance of the receiver from the axis of the cable along the seafloor in terms of skin depths of seawater. Each curve corresponds to a different value of $R$ ($R = (\sigma_f/\sigma_s)^{1/2}$); $R$ takes the values of 0.01, 0.03, 0.1, 0.3, and 1 except for the $B_{s,y}^p$ component which is zero when $R = 1$ (no seafloor). Both axes are plotted on a logarithmic scale.

The second panels in Figures 3 and 5 show the variations of the amplitude ratio of $E_{s,x}$ and $B_{s,z}$ produced on the seafloor to those produced in a sea of infinite depth as a function of distance. The second panel in Figure 4 plots the variation of the ratio of the amplitude of $B_{s,y}$ to the amplitude of $B_{s,z}$ as a function of distance.

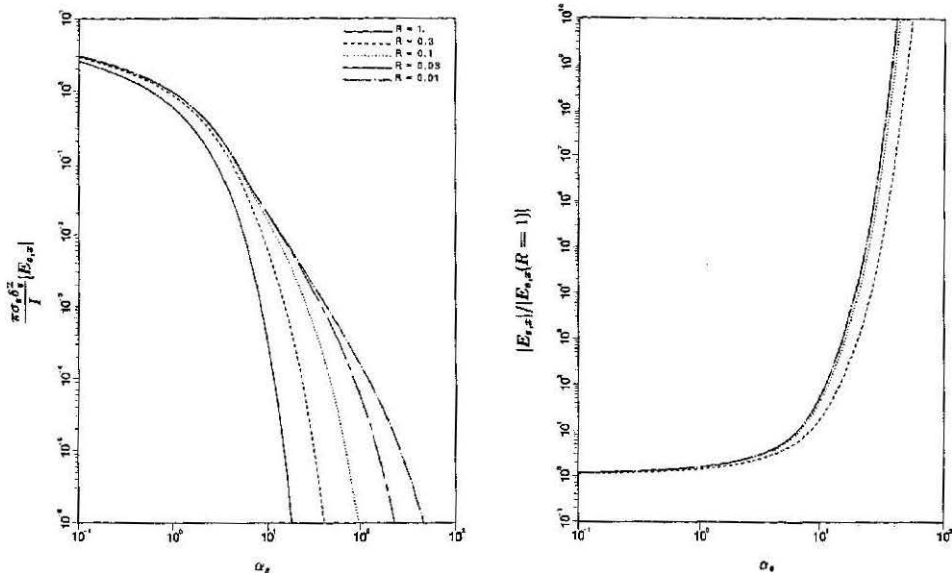In Figures 7 and 8, the real amplitudes of the field

Fig. 3. Variations in the amplitude of the electric field produced on the seafloor by an infinite cable and variation of the ratio curves illustrating the changes in the total electric field in the case of an electrically conducting seabed as a function of distance. Each curve corresponds to a different seabed conductivity. The curves in the second panel show the ratio of the amplitudes of the electric field at the seafloor interface to the electric field in an infinitely deep sea.
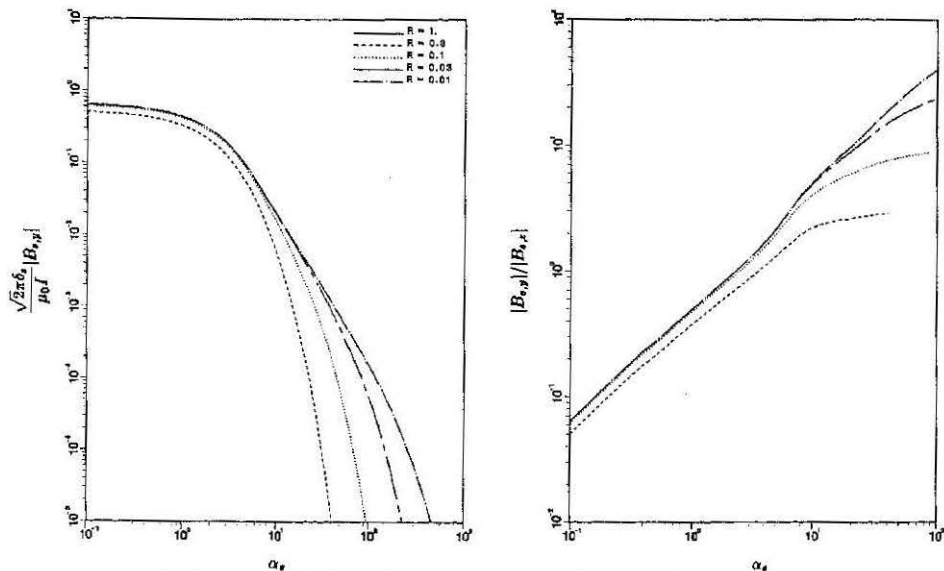


Fig. 4. Variation in the amplitude of the horizontal component of the magnetic field produced on the seafloor by an infinite cable and variation of the ratio of the amplitudes of the horizontal component to the vertical component of the magnetic field, both produced on the seafloor by an infinite cable in the case of an electrically conducting seabed. Each curve is a function of distance and corresponds to a different seabed conductivity.
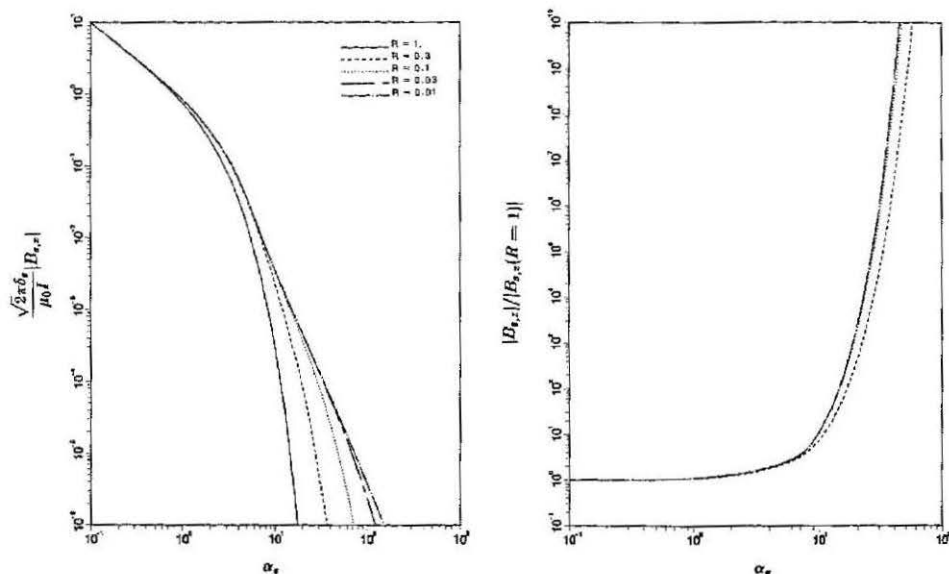
Fig. 5. Variation of the amplitude of the vertical component of the magnetic field produced on the seafloor by an infinite cable and variation of the ratio illustrating the changes in the vertical component of the field in the case of an electrically conducting seabed as a function of distance. Each curve corresponds to a different seabed conductivity. The curves in the second panel show the ratio of the amplitudes of the vertical component of the magnetic field produced on the seafloor to the same component in an infinitely deep sea.
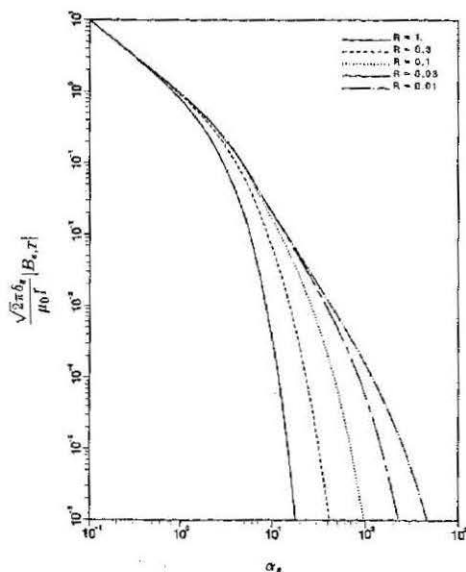


components $E_{s,x}$, $B_{s,y}$, $B_{s,z}$ and the total magnetic field $B_{s,T}$ are plotted vs distance for an alternating current source with an amplitude of 1000 A and a frequency of 1 Hz for the above seafloor conductivities. The units of the electric and magnetic fields are milivolts/meter and picotesla, and distance is in meters.

The above results can be plotted in another parametric form in which the amplitude of the field components is written as

$$|E_{s,x}^p|_y = \frac{2\pi\sigma_s y^2}{I}|E_{s,x}| \tag{13}$$

$$|B_{s,(y,z,T)}^p|_y = \frac{2\pi y}{\mu_0 I}|B_{s,(y,z,T)}| \tag{14}$$

Here, the terms on the left-hand side are not functions of frequency but, instead, are functions of receiver distance $y$. Figures 9 and 10 plot the variations of the field components in (13) and (14), and

Fig. 6. Variation with distance of the amplitude of the total magnetic field produced on the seafloor by an infinite cable. Each curve corresponds to a different seabed conductivity.
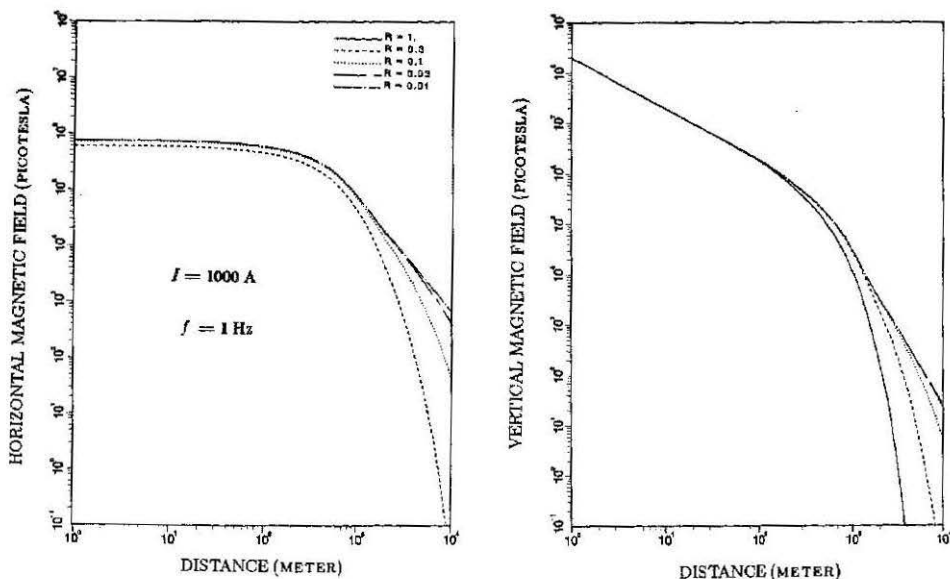
Fig. 7. Variations in the amplitudes of the horizontal and vertical components of the magnetic field produced on the seafloor by an infinite cable carrying an alternating current with an amplitude of 1000 A and a frequency of 1 Hz as a function of distance. Each curve corresponds to a different seabed conductivity.

the horizontal axis shows the variation in frequency. Note, once again, that each curve corresponds to a different seabed conductivity and there is no horizontal magnetic field component for $R = 1$.

## 4. DISCUSSION

All three field components produced at the interface can propagate farther when a seafloor is present than can those produced in the absence of a seafloor because of the assumed lower conductivity of the seabed. The increase in range becomes significant at greater distances. For example, when $f = 1$ Hz, the amplitude of the horizontal component of the electric field $E_{s,x}$ becomes 1 nV/m at a distance of $y \simeq 3$ km for $\sigma' = 1$ (infinitely deep sea), $y \simeq 18$ km for $\sigma' = 10^{-2}$, and $y \simeq 90$ km for $\sigma' = 10^{-4}$. At 90 km, the source cable must be much longer for it to be an infinite cable; for example, if it is 10 times longer (900 km), a uniform current distribution is still a good assumption at 1 Hz [Inan et al., 1983].

The horizontal component of the magnetic field $B_{s,y}$ is negligible when compared to the vertical component $B_{s,z}$ near the cable; however, it becomes comparable to and larger than $B_{s,z}$ at greater receiver distances (Figure 4). For example, if $I = 1000$ A,

$f = 1$ Hz, and $\sigma' = 0.01$, the amplitudes of the horizontal and vertical magnetic field components would be $|B_{s,y}| \simeq 0.70 \times 10^6$ pT and $|B_{s,z}| \simeq 0.20 \times 10^8$ pT at 10 m, $0.57 \times 10^6$ and $0.19 \times 10^7$ pT at 100 m, and $0.68 \times 10^5$ and $0.30 \times 10^5$ pT at 1 km. The amplitude of $B_{s,y}$ is also more sensitive to the conductivity of the seabed than are the amplitudes of the other two field components $E_{s,x}$ and $B_{s,z}$.

The horizontal component of the magnetic field and the electric field are zero when $\omega = 0$. They also have optimal frequencies as observed in Figure 9; for example, at a distance of 1 km, the electric field has an optimal frequency of approximately 0.15 Hz in an infinitely deep sea [Inan et al., 1983].

## 5. APPLICATIONS

The numerical results obtained in this work could be useful in the area of undersea communication. The range of communication with submersibles in the deep parts of the ocean is limited because of the high conductivity of the seawater. The seabed has an effective conductivity smaller than that of seawater and, as a result, it may provide a new path for the signals along which there will be less attenuation compared to a signal propagating directly through
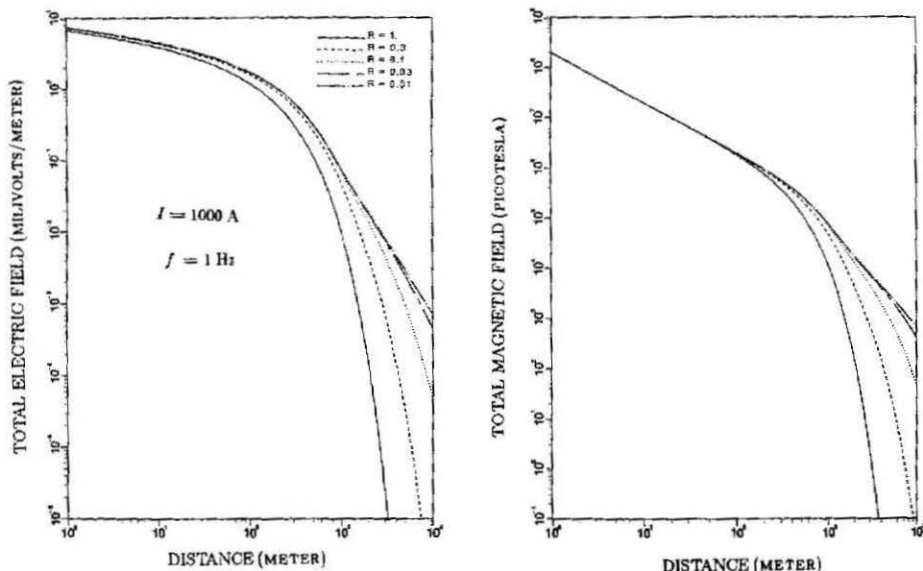
Fig. 8. Variations in the amplitudes of the total electric and magnetic fields produced on the seafloor by an infinite cable carrying an alternating current with an amplitude of 1000 A and a frequency of 1 Hz as a function of distance. Each curve corresponds to a different seabed conductivity.

seawater; longer ranges can be achieved before the signal becomes weak and cannot be detected because of external and internal receiver noise. The seabed is also a conducting medium and the exponential attenuation of electromagnetic signals propagating through the seabed is still significantly large at high frequencies; therefore, operating frequencies must be low enough to reach long ranges. This limits the bandwidth, and information cannot be transferred at a high data rate.

New components at the seafloor interface will increase the ranges of communication. For an infinite cable carrying an alternating current of 1000 A at 1 Hz and assuming the minimum measurable magnetic field to be 0.1 pT, the field on the seafloor can be detected over a range of approximately 4 km before its amplitude drops below 0.1 pT. The amplitudes of the new horizontal component and the vertical component of the magnetic field along the interface are 0.24 and 0.09 pT at a receiver distance of 8 km for an effective seabed conductivity of 0.4 S/m, and the total magnetic field of 0.26 pT. If the seabed conductivity is 0.04 S/m, the two field components are 0.27 and 0.03 pT at a receiver distance of 20 km, and the total magnetic field becomes 0.27 pT as a result of this

new component. These two components are about $0.39 \times 10^3$ and $0.22 \times 10^2$ pT at 20 km for a seabed conductivity of 0.004 S/m. These examples indicate that the range of electromagnetic fields along the seafloor increases significantly before their amplitudes drop below the minimum measurable field value.

Arrays of long cables located on the seafloor can achieve longer communication ranges [Inan et al., 1982]. The phases of the currents in each cable can be adjusted to produce a maximum field amplitude at the receiver, which makes communication possible over a much larger area. The separation distance of the cables depends on the current amplitudes, frequency, conductivity of the seabed, sensitivity of the receiver, and background noise. With a series array of cables, each carrying an alternating current of amplitude 1000 A and frequency 1 Hz and separated from each other by 30 skin depths, the magnetic field produced at a point midway between the two cables would be approximately $4 \times 10^2/\delta_s$ or 1.6 pT in an infinitely deep sea; on a seabed with $\sigma_f = 0.04$ S/m, this field would be $4.6 \times 10^3$ pT. The results indicate that the cables moved apart from a spacing of $30\delta_s$ to $140\delta_s$ would yield the same field produced in an infinitely deep sea at that point. Large amounts of re-
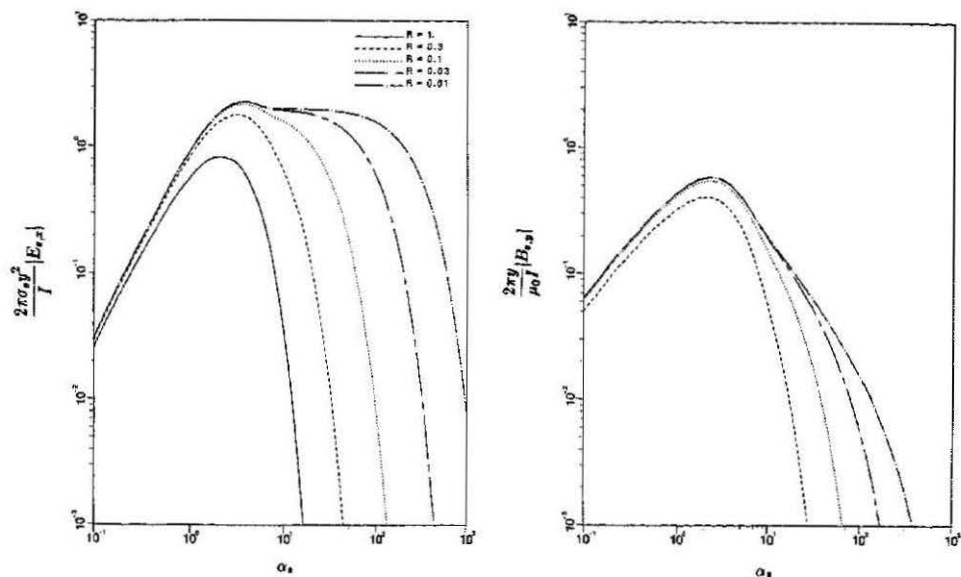
Fig. 9. Variations in the amplitudes of the electric field and horizontal component of the magnetic field produced on the seafloor by an infinite cable carrying an alternate current as a function of frequency. Each curve corresponds to a different seabed conductivity.
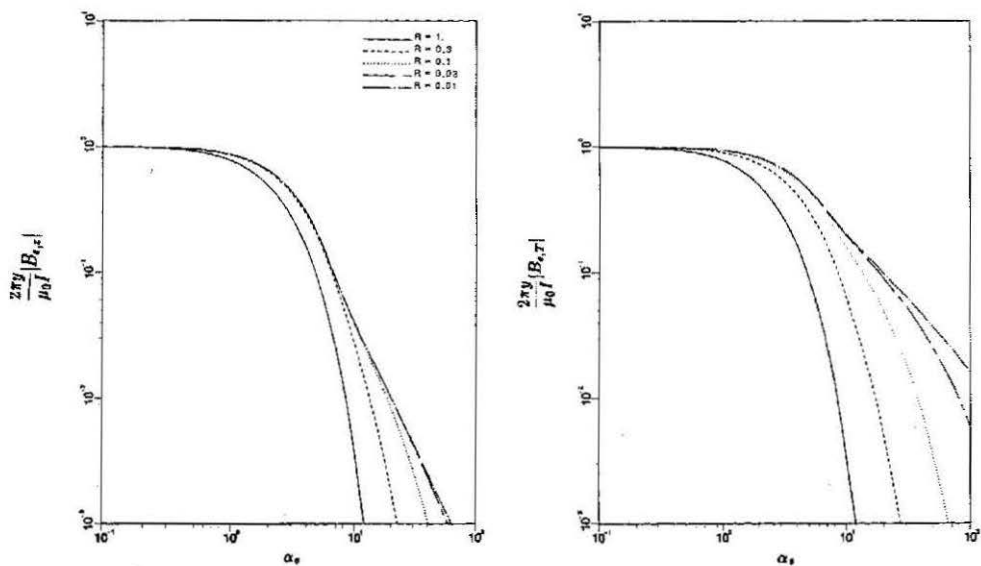


Fig. 10. Variations in the amplitudes of the vertical component of the magnetic field and the total magnetic field produced on the seafloor by an infinite cable carrying an alternate current as a function of frequency. Each curve corresponds to a different seabed conductivity.
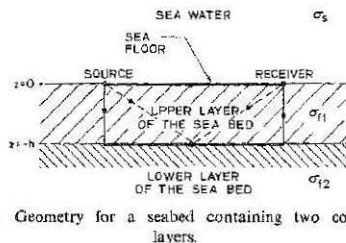
Fig. 11. Geometry for a seabed containing two conducting layers.

sistive power will be lost, however, as the source current flows in both the long cables and surrounding conducting media. The advantage of this system is a less noisy environment in which the electromagnetic signals propagate, because atmospheric noise at these low frequencies will be shielded by the large depth of seawater [*Mott and Biggs,* 1963].

## 6. RECOMMENDATIONS

Throughout this investigation, it has been assumed that the seabed is a homogenous medium; however, it often contains layers of sediment with different properties. This work could be extended to two or more layers. For example, in the two-layer bed in Figure 11, the first layer has a conductivity of $\sigma_{f1}$ and extends from $z = 0$ to $z = -h$ and the second has a conductivity of $\sigma_{f2}$ and extends from $z = -h$ to $z = -\infty$. Both the source and receiver are located at the sea/seabed interface. The conductivity of the upper layer is in general larger than that of the lower layer. For receiver distances smaller than the depth of the first layer, the effects of the low-conductivity layer should not be very significant. As receiver distances become larger than the depth of the first layer, however, the signal that follows the down-under-up mode will be much stronger than the signal that directly propagates from the source to the receiver using the sea/seabed boundary, and the lower layer will be important. This means that, depending on the location of the observer, the signal at the receiver will carry information about the properties of different layers of the seabed.

The length of the straight cable was assumed to be infinite. This is a good assumption for a receiver located in the vicinity of the cable (where the perpendicular distance to the receiver is much smaller than the actual length of the straight cable) and not close to the ends of the cable. A uniform current distribution along the cable was also assumed. Although this is not true in an infinite cable, the fields produced at the receiver will be the result of the middle

portion of the cable because the contribution from the portions toward the ends (not necessarily carrying the same current) will be negligible. As the receiver distance increases, however, a longer portion of the cable must be considered and the uniform-current assumption may no longer be valid. One extension of this work would be to calculate the distribution of the current along a long straight insulated cable located at the seafloor interface.

In practice, it may not be possible to locate the receiver precisely at the interface. Another extension would be to place the receiver some distance above the sea/seabed interface and then calculate the fields in this configuration. The integrals for the field expressions will then require an additional term $e^{-u_s z}$ representing the exponential attenuation as the signal is propagating the vertical distance between the source and receiver in the seawater. As a result, the fields produced at some vertical distance above the seafloor will generally be smaller in amplitude than the fields produced on the seafloor.

In concluding, we should comment on the dispersion that is likely to be involved in the propagation of ULF/ELF fields along the seafloor. Because of their conductivity, both the sea and seabed are dispersive and there will therefore be a limit on the achievable transmission bandwidth (i.e., on the amount of information that can be transmitted). To illustrate, let us consider a carrier frequency of 100 Hz modulated at 1 Hz, 10 Hz, and 100 Hz (i.e., with 1%, 10%, and 100% bandwidths). We will assume, for simplicity, that the amplitudes of all the frequency components that fall into this frequency band are equal and attenuated at the same rate. The phase difference between the two extreme frequency components (the upper and the lower sidebands) propagating through seawater becomes 180° at distances of 15.8 km, 1.58 km, and 152.7 m, respectively. If the carrier frequency is 1 kHz with the same percent bandwidths, the phase difference becomes 180° at distances of 5 km, 500 m, and 48.3 m, respectively. These results show that the transmission range must be reduced as the bandwidth is made larger if the effects of dispersion are to be minimized. Another related conclusion follows immediately from the $f^{1/2}$ dependence of phase velocity on frequency: if the carrier frequency is decreased the bandwidth also must be reduced if an increase of dispersion is to be avoided. Finally, propagation through the seabed has a decided advantage over propagation through the sea from the point of view of reduced dispersion as well as increased range. Once again taking an illus-

trative example, suppose the seabed conductivity is 0.04 S/m and we apply the conditions in the example above to propagation through the seabed instead of the sea. In the seabed the ranges are all ten times greater than those in seawater.

## REFERENCES

Bannister, P. R., Determination of the electrical conductivity of the sea bed in shallow waters, Geophysics, 33, 995–1003, 1968a.

Bannister, P. R., Electromagnetic fields within a stratified earth produced by a long horizontal line source, Radio Sci., 3, 387–390, 1968b.

Bannister, P. R., and R. L. Dube, Numerical results for modified image theory quasi-static range subsurface-to-subsurface and subsurface-to-air propagation equations, Tech. Rep. 5775, 30 pp., Nav. Underwater Syst. Cent., New London, Conn., 1977.

Banos, A., Dipole Radiation in the Presence of a Conducting Half Space, 245 pp., Pergamon, New York, 1966.

Brock-Nannestad, L., Determination of the electrical conductivity of the seabed in shallow waters with varying conductivity profile, Electron. Lett., 1, 274–276, 1965.

Bubenik, D. M., and A. C. Fraser-Smith, ULF/ELF electromagnetic fields generated in a sea of finite depth by a submerged vertically-directed harmonic magnetic dipole, Radio Sci., 13, 1011–1020, 1978.

Burrows, C. R., Radio communication within the earth's crust, IEEE Trans. Antennas Propag., AP-11, 311–317, 1963.

Butterworth, S., The distribution of the magnetic field and return current round a submarine cable carrying alternating current, 2, Philos. Trans. R. Soc. London, Ser. A, 224, 141–184, 1924.

Chave, A. D., and C. S. Cox, Controlled electromagnetic sources for measuring electrical conductivity beneath the oceans, 1, Forward problem and model study, J. Geophys. Res., 87, 5327–5338, 1982.

Coggon, J. H., and H. F. Morrison, Electromagnetic investigation of the sea floor, Geophysics, 35, 476–489, 1970.

Computation Laboratory of Harvard University, Tables of the Generalized Exponential-Integral Functions, 416 pp., Harvard University Press, Cambridge, Mass., 1949.

Drysdale, C. V., The distribution of the magnetic field and return current round a submarine cable carrying alternating current, 1, Philos. Trans. R. Soc. London, Ser. A, 224, 95–140, 1924.

Fraser-Smith, A. C., and D. M. Bubenik, ULF/ELF electromagnetic fields generated at the sea surface by submerged magnetic dipoles, Radio Sci., 11, 901–913, 1976.

Fraser-Smith, A. C., and D. M. Bubenik, ULF/ELF electromagnetic fields generated above a sea of finite depth by a submerged vertically-directed harmonic magnetic dipole, Radio Sci., 14, 59–74, 1979.

Hansen, R. C., Radiation and reception with buried and submerged antennas, IEEE Trans. Antennas Propag., AP-11, 207–216, 1963.

Hermance, J. F., and W. R. Peltier, Magnetotelluric fields of a line current, J. Geophys. Res., 75, 3351–3356, 1970.

Inan, A. S., A. C. Fraser-Smith, and O. G. Villard, Jr., ULF/ELF electromagnetic fields produced in sea water by linear current sources, Tech. Rep. E721-1, 104 pp., Stanford Electron. Lab., Stanford Univ., Calif., 1982.

Inan, A. S., A. C. Fraser-Smith, and O. G. Villard, Jr., ULF/ELF electromagnetic fields produced in a conducting medium of infinite extent by linear current sources of infinite length, Radio Sci., 18, 1383–1392, 1983.

King, R. W. P., and G. S. Smith, Antennas in Matter, sect. 11.12, MIT Press, Cambridge, Mass., 1981.

Kraichman, M. B., Handbook of Electromagnetic Propagation in Conducting Media, U.S. Government Printing Office, Washington, D. C., 1976.

Liebermann, L. N., Other electromagnetic radiation, in The Sea, vol. 1, Physical Oceanography, edited by M. N. Hill, chap. 11, John Wiley, New York, 1962.

Lowell, H. H., Tables of the bessel-kelvin functions ber, bei, ker, kei, and their derivatives for the argument range 0(0.01)107.50, NASA Tech. Rep., R-32, 296 pp., 1959.

Moore, R. K., The theory of radio communication between submerged submarines, Ph.D. thesis, Cornell Univ., Ithaca, N. Y., 1951.

Moore, R. K., Radio communication in the sea, IEEE Spectrum, 4, 42–51, 1967.

Moore, R. K., and W. E. Blair, Dipole radiation in a conducting half-space, J. Res. Natl. Bur. Stand., Sect. D, 65D, 547–563, 1961.

Mott, H., and A. W. Biggs, Very-low-frequency propagation below the bottom of the sea, IEEE Trans. Antennas Propag., AP-11, 323–329, 1963.

Pickard, G. L., and W. J. Emery, Descriptive Physical Oceanography, An Introduction, Fourth Enlarged Edition, 249 pp., Pergamon, New York, 1982.

Ramaswamy, V., H. S. Dosso, and J. T. Weaver, Horizontal magnetic dipole embedded in a two-layer conducting medium, Can. J. Phys., 50, 607–616, 1972.

Soderberg, E. F., ELF noise in the sea at depths from 30 to 300 meters, J. Geophys. Res., 74, 2376–2387, 1969.

Sunde, E. D., Earth Conduction Effects in Transmission Systems, 370 pp., Dover, New York, 1968.

Tranter, C. J., Integral Transforms in Mathematical Physics, pp. 67–72, Methuen, London, 1956.

Wait, J. R., Electromagnetic fields of current-carrying wires in a conducting medium, Can. J. Phys., 30, 512–523, 1952.

Wait, J. R., The fields of a line source of current over a stratified conductor, Appl. Sci. Res., Sect. B, 3, 279–292, 1953.

Wait, J. R., The electromagnetic fields of a horizontal dipole in the presence of a conducting half-space, Can. J. Phys., 39, 1017–1028, 1961.

Wait, J. R., Electromagnetic Waves in Stratified Media, chap. 2, Pergamon, New York, 1962.

Wait, J. R., Project Sanguine, Science, 178, 272–275, 1972.

Wait, J. R., and L. L. Campbell, The fields of an oscillating magnetic dipole immersed in a semi-infinite conducting medium, J. Geophys. Res., 58, 167–178, 1953.

Wait, J. R., and K. P. Spies, Electromagnetic propagation in an idealized earth crust waveguide, I, Pure Appl. Geophys., 101, 174–187, 1972a.

Wait, J. R., and K. P. Spies, Electromagnetic propagation in an idealized earth crust waveguide, II, Pure Appl. Geophys., 101, 188–193, 1972b.

Wait, J. R., and K. P. Spies, Dipole excitation of ultra-low-frequency electromagnetic waves in the earth crust waveguide, J. Geophys. Res., 77, 7118–7120, 1972c.

Wait, J. R., and K. P. Spies, Subsurface electromagnetic fields of a line source on a two-layer conducting earth, Radio Sci., 8, 805–810, 1973.

Weaver, J. T., The quasi-static field of an electric dipole embedded in a two-layer conducting half-space, Can. J. Phys., 45, 1981–2002, 1967.

Wheeler, H. A., Radio-wave propagation in the earth's crust, *J. Res. Natl. Bur. Stand. Sect. D*, 65D, 189–191, 1960.

Wright, C., Leader gear, in *Proceedings of Symposium on Underwater Electromagnetic Phenomena*, edited by G. W. Wood, pp. 177–184, National Academy of Sciences National Research Council, Washington, D. C., 1953.

Young, A., and A. Kirk, Bessel functions, 4, Kelvin functions, *R. Soc. Math. Tables, 10*, 97 pp., 1964.

Young, P. D., and C. S. Cox, Electromagnetic active source sounding near the East Pacific Rise, *Geophys. Res. Lett., 8*, 1043–1046, 1981.

A. C. Fraser-Smith and O. G. Villard, Jr., STAR Laboratory, Department of Electrical Engineering/Space Environment Laboratory, Stanford University, Stanford, CA 94305.

A. S. Inan, Engineering Department, San Francisco State University, 1600 Holloway Avenue, San Francisco, CA 94132.